Nonequilibrium Spin-Glass Dynamics from Picoseconds to a Tenth of a Second

F. Belletti,[1] M. Cotallo,[2] A. Cruz,[3,2] L. A. Fernandez,[4,2] A. Gordillo-Guerrero,[5,2] M. Guidetti,[1] A. Maiorano,[1,2] F. Mantovani,[1] E. Marinari,[6] V. Martin-Mayor,[4,2] A. Muñoz Sudupe,[4] D. Navarro,[7] G. Parisi,[6] S. Perez-Gaviro,[2] J. J. Ruiz-Lorenzo,[5,2] S. F. Schifano,[1] D. Sciretti,[2] A. Tarancon,[3,2] R. Tripiccione,[1] J. L. Velasco,[2] and D. Yllanes[4,2]

[1]*Dipartimento di Fisica Università di Ferrara and INFN - Sezione di Ferrara, Ferrara, Italy*
[2]*Instituto de Biocomputación y Física de Sistemas Complejos (BIFI), Zaragoza, Spain*
[3]*Departamento de Física Teórica, Universidad de Zaragoza, 50009 Zaragoza, Spain*
[4]*Departamento de Física Teórica I, Universidad Complutense, 28040 Madrid, Spain*
[5]*Departamento de Física, Universidad de Extremadura, 06071 Badajoz, Spain*
[6]*Dipartimento di Fisica, INFM and INFN, Università di Roma "La Sapienza", 00185 Roma, Italy*
[7]*D. de Ingeniería, Electrónica y Comunicaciones and I3A, U. de Zaragoza, 50018 Zaragoza, Spain*
(Received 11 April 2008; revised manuscript received 23 June 2008; published 6 October 2008)

We study numerically the nonequilibrium dynamics of the Ising spin glass, for a time spanning 11 orders of magnitude, thus approaching the experimentally relevant scale (i.e., *seconds*). We introduce novel analysis techniques to compute the coherence length in a model-independent way. We present strong evidence for a replicon correlator and for overlap equivalence. The emerging picture is compatible with noncoarsening behavior.

DOI: 10.1103/PhysRevLett.101.157201 PACS numbers: 75.10.Nr, 75.40.Gb, 75.40.Mg, 75.50.Lk

Spin glasses [1] (SG) exhibit remarkable features, including slow dynamics and a complex space of states: they are a paradigmatic problem because of its many applications to glassy behavior, optimization, biology, financial markets, social dynamics, etc.

Experiments on SG [1,2] focus on nonequilibrium dynamics. In the simplest protocol, isothermal aging, the SG is cooled as fast as possible to a subcritical working temperature, $T < T_c$, let to equilibrate for a *waiting time*, t_w, and probed at a later time, $t + t_w$. The thermoremanent magnetization is found to be a function of t/t_w (*full aging*), for $10^{-3} < t/t_w < 10$ and $50\ \mathrm{s} < t_w < 10^4\ \mathrm{s}$ [3] (see, however, [4]). The growing size of the coherent domains, the coherence-length ξ, is also measured [5,6]. Two features emerge: (i) the lower T, the slower the growth of $\xi(t_w)$ and (ii) $\xi \sim 100$ lattice spacings, even for $T \sim T_c$ and $t_w \sim 10^4$ s [5].

The sluggish dynamics arises from a thermodynamic transition at T_c [7–9]. There is a sustained theoretical debate on the properties of the (unreachable in human times) equilibrium low T SG phase, which is nevertheless relevant to (basically nonequilibrium) experiments [10]. The main scenarios are the droplets [11], replica symmetry breaking (RSB) [12], and the intermediate trivial-nontrivial (TNT) picture [13].

Droplets expects two equilibrium states related by global spin reversal. The SG order parameter, the spin overlap q, takes only two values $q = \pm q_{\mathrm{EA}}$. In the RSB scenario an infinite number of pure states influence the dynamics [12,14,15], so all $-q_{\mathrm{EA}} \leq q \leq q_{\mathrm{EA}}$ are reachable. In TNT the SG phase is similar to an antiferromagnet with random boundary conditions: q behaves as for RSB systems but, similar to droplets, the surface-to-volume ratio of the largest thermally activated domains vanishes (i.e., the link-overlap defined below takes a single value).

Because of superuniversality [16], the isothermal aging of basically all coarsening systems is qualitatively the same (droplets being analogous to a disguised ferromagnet [17]). For $T < T_c$ the dynamics consists in the growth of compact domains, where the spin overlap takes one of the values $q = \pm q_{\mathrm{EA}}$. The corresponding growth law, $\xi(t)$, completely encodes all time dependencies. The antiferromagnet analogy suggests a similar TNT aging.

Since in the RSB scenario $q = 0$ equilibrium states do exist, the nonequilibrium dynamics starts with a vanishing order parameter and remains there forever. The replicon, a critical mode analogous to magnons in Heisenberg ferromagnets, is present for all $T < T_c$ [18]. Furthermore, q is not a privileged observable (overlap equivalence [14]): the link overlap displays equivalent aging behavior.

These theories need numerics to be quantitative [19–27]. Simulations so far have been too short: experimental scales are at $\sim$100 s, while typical nonequilibrium simulations reach $\sim 10^{-5}$ s (one Monte Carlo step, MCS, corresponds to 10^{-12} s [1]). Over the years, high-performance computers have been built for SG simulations [28–30].

Here we report on a large simulation (10^{11} MCS $\sim$ 0.1 s) of an instantaneous SG quench protocol performed on the Janus computer [30], which allows us to reach experimental times by mild extrapolations. Aging is investigated as a function of time and temperature. We obtain model-independent determinations of the SG coherence length ξ. Conclusive evidence is presented for a critical correlator associated with the replicon mode. We observe nontrivial aging in the link correlation (a *nonequilibrium* test of overlap equivalence [14]). We conclude that, up to experimental scales, SG dynamics is not coarsening like.

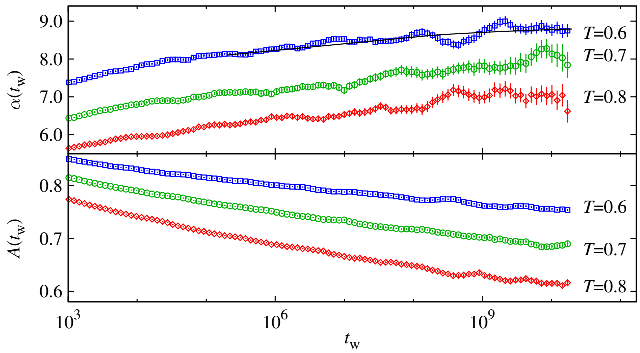

FIG. 1 (color online). Fit parameters, A and α ($C(t, t_w) = A(t_w)(1 + t/t_w)^{-1/\alpha(t_w)}$) vs t_w for temperatures below T_c ($T = 0.6$ line: fit, for $t_w > 10^5$, to $\alpha(t_w) = \alpha_0 + \alpha_1 \log t_w + \alpha_2 \log^2 t_w$, $\alpha_0 = 6.357\,95$, $\alpha_1 = 0.186\,05$, $\alpha_2 = -0.003\,518\,35$, diagonal $\chi^2/\text{d.o.f.} = 66.26/63$). Oscillations are due to strong correlations of $\alpha(t_w)$ at neighboring times (the fit and $\chi^2/\text{d.o.f.}$ do not change if we bin data in blocks of 5 consecutive t_w).

The $D = 3$ Edwards-Anderson Hamiltonian is

$$\mathcal{H} = -\sum_{\langle \boldsymbol{x}, \boldsymbol{y} \rangle} J_{\boldsymbol{x},\boldsymbol{y}} \sigma_{\boldsymbol{x}} \sigma_{\boldsymbol{y}}, \tag{1}$$

($\langle \cdots \rangle$ denote nearest neighbors). Spins $\sigma_{\boldsymbol{x}} = \pm 1$ sit at the nodes, $\boldsymbol{x}$, of a cubic lattice of size L and periodic boundary conditions. The couplings (quenched variables) $J_{\boldsymbol{x},\boldsymbol{y}} = \pm 1$ are chosen randomly with 50% probability. For each set of couplings (a sample), we simulate two independent systems, $\{\sigma_{\boldsymbol{x}}^{(1)}\}$ and $\{\sigma_{\boldsymbol{x}}^{(2)}\}$. We denote by $\overline{(\cdots)}$ the average over the couplings. Model (1) has a SG transition at $T_c = 1.101(5)$ [31].

Our $L = 80$ systems evolve with Heat-Bath dynamics [32], which is in the Universality Class of physical evolution. Fully disordered starting spin configurations are placed at the working temperature (96 samples at $T = 0.8 \approx 0.73 T_c$ and at $T = 0.6 \approx 0.54 T_c$; 64 at $T = 0.7 \approx 0.64 T_c$). We also perform shorter simulations (32 samples) at T_c, and $L = 40$ and $L = 24$ runs to check for finite-size effects.

A crucial quantity is the two-times correlation function [19,20,23]: $[c_{\boldsymbol{x}}(t, t_w) \equiv \sigma_{\boldsymbol{x}}(t + t_w)\sigma_{\boldsymbol{x}}(t_w)]$

$$C(t, t_w) = \overline{L^{-3} \sum_{\boldsymbol{x}} c_{\boldsymbol{x}}(t, t_w)}, \tag{2}$$

linearly related to the real part of the a.c. susceptibility at waiting time t_w and frequency $\omega = \pi/t$.

To check for full aging [3] in a systematic way, we fit $C(t, t_w)$ as $A(t_w)(1 + t/t_w)^{-1/\alpha(t_w)}$ in the range $t_w \le t \le 10 t_w$ [33], obtaining fair fits for all $t_w > 10^3$; see Fig. 1. To be consistent with the experimental claim of full-aging behavior for $10^{14} < t_w < 10^{16}$ [3], $\alpha(t_w)$ should be constant in this t_w range. Although $\alpha(t_w)$ keeps growing for our largest times (with the large errors in [23] it seemed constant for $t_w > 10^4$), its growth slows down. The behavior at $t_w = 10^{16}$ seems beyond reasonable extrapolation.

The coherence length is studied from the correlations of the replica field $q_{\boldsymbol{x}}(t_w) \equiv \sigma_{\boldsymbol{x}}^{(1)}(t_w)\sigma_{\boldsymbol{x}}^{(2)}(t_w)$,

$$C_4(\boldsymbol{r}, t_w) = \overline{L^{-3} \sum_{\boldsymbol{x}} q_{\boldsymbol{x}}(t_w) q_{\boldsymbol{x}+\boldsymbol{r}}(t_w)}. \tag{3}$$

For $T < T_c$, it is well described by [12,21]

$$C_4(\boldsymbol{r}, t_w) \sim r^{-a} e^{-(r/\xi(t_w))^b}, \qquad a \simeq 0.5, \qquad b \simeq 1.5. \tag{4}$$

The actual value of a is relevant. For coarsening dynamics $a = 0$, while in a RSB scenario $a > 0$ and $C_4(r, t_w)$ vanishes at long times for fixed $r/\xi(t_w)$. At T_c, the latest estimate is $a = 1 + \eta = 0.616(9)$ [31].

To study a independently of a particular Ansatz as (4) we consider the integrals

$$I_k(t_w) = \int_0^\infty \mathrm{d}r\, r^k C_4(r, t_w), \tag{5}$$

(e.g., the SG susceptibility is $\chi^{\mathrm{SG}}(t_w) = 4\pi I_2(t_w)$). As we assume $L \gg \xi(t_w)$ we safely reduce the upper limit to $L/2$. If a scaling form $C_4(r, t_w) \sim r^{-a} f[r/\xi(t_w)]$ is adequate at large r, then $I_k(t_w) \propto [\xi(t_w)]^{k+1-a}$. It follows that $\xi_{k,k+1}(t_w) \equiv I_{k+1}(t_w)/I_k(t_w)$ is proportional to $\xi(t_w)$ and $I_1(t_w) \propto \xi_{k,k+1}^{2-a}$. We find $\xi^{(2)}(t_w) \approx 0.8 \xi_{1,2}(t_w)$, where $\xi^{(2)}$ is the noisy second-moment estimate [9]. Furthermore, for $\xi_{1,2} > 3$, we find $\xi_{0,1}(t_w) \approx 0.46 \xi_{1,2}(t_w)$, and $\xi^{\mathrm{fit}}(t_w) = 1.06 \xi_{1,2}(t_w)$, ($\xi^{\mathrm{fit}}$ from a fit to (4) with $a = 0.4$).

Note that, when $\xi \ll L$, irrelevant distances $r \gg \xi$ largely increase statistical errors for I_k. Fortunately, the very same problem was encountered in the analysis of correlated time series [34], and we may borrow the cure [35].

The largest t_w where $L = 80$ still represents $L = \infty$ physics follows from finite-size scaling [32]: for a given

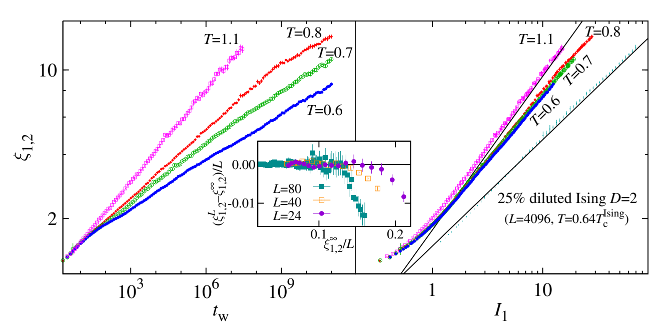

FIG. 2 (color online). Left: SG coherence length $\xi_{1,2}$ vs waiting time, for $T \le T_c$. Right: $\xi_{1,2}$ vs I_1, ($\xi_{1,2} \propto I_1^{1/(2-a)}$). Also shown data for the site-diluted Ising model ($\xi_{1,2}$ and I_1 rescaled by 2). Full lines: Ising (coarsening, $a = 0$) and SG, $a(T_c) = 0.616$ [31]. Inset: $[\xi_{1,2}^L(t_w) - \xi_{1,2}^\infty(t_w)]/L$ vs $\xi_{1,2}^\infty(t_w)/L$ for $T = 0.8$ and $L = 24$, 40 and 80 ($\xi_{1,2}^\infty(t_w)$ from a fit $\xi_{1,2}(t_w) = A(T) t_w^{1/z(T)}$ for $L = 80$ in the range $3 < \xi_{1,2} < 10$).

numerical accuracy, one should have $L \geq k\xi_{1,2}(t_w)$. To compute k, we compare $\xi^L_{1,2}$ for $L = 24$, 40 and 80 with $\xi^\infty_{1,2}$ estimated with the power law described below (Fig. 2, inset). It is clear that the safe range is $L \geq 7\xi_{1,2}(t_w)$ at $T = 0.8$ (at T_c the safety bound is $L \geq 6\xi_{1,2}(t_w)$).

Our results for $\xi_{1,2}$ are shown in Fig. 2. Note for $T = 0.8$ the finite-size change of regime at $t_w = 10^9 (\xi_{1,2} \sim 11)$. We find fair fits to $\xi(t_w) = A(T)t_w^{1/z(T)}$: $z(T_c) = 6.86(16)$, $z(0.8) = 9.42(15)$, $z(0.7) = 11.8(2)$ and $z(0.6) = 14.1(3)$, in good agreement with previous numerical and experimental findings $z(T) = z(T_c)T_c/T$ [5,21]. Our fits are for $3 \leq \xi \leq 10$, to avoid both finite-size and lattice discretization effects. Extrapolating to experimental times ($t_w = 10^{14} \sim 100$ s), we find $\xi = 14.0(3)$, 21.2(6), 37.0(14), and 119(9) for $T = 0.6$, $T = 0.7$, $T = 0.8$ and $T = 1.1 \approx T_c$, respectively, which nicely compares with experiments [5,6].

In Fig. 2, we also explore the scaling of I_1 as a function of $\xi_{1,2}$ ($I_1 \propto \xi^{2-a}$). The nonequilibrium data for $T = 1.1$ scales with $a = 0.585(12)$. The deviation from the *equilibrium* estimate $a = 0.616(9)$ [31] is at the limit of statistical significance (if present, it would be due to scaling corrections). For $T = 0.8$, 0.7, and 0.6, we find $a = 0.442(11)$, 0.355(15), and 0.359(13), respectively (the residual T dependence is probably due to critical effects still felt at $T = 0.8$). Note that ground state computations for $L \leq 14$ yielded $a(T = 0) \approx 0.4$ [37]. These numbers differ both from critical and coarsening dynamics ($a = 0$).

We finally address the aging properties of $C_{\text{link}}(t, t_w)$

$$C_{\text{link}}(t, t_w) = \overline{\sum_{\langle \boldsymbol{x}, \boldsymbol{y}\rangle} c_{\boldsymbol{x}}(t, t_w) c_{\boldsymbol{y}}(t, t_w)}/(3L^3). \tag{6}$$

C_{link}, still experimentally inaccessible, does not vanish if the configurations at $t + t_w$ and t_w differ by the spin inversion of a compact region of half the system size.

It is illuminating to replace t with $C^2(t, t_w)$ as an independent variable; Figs. 3 and 4. For a coarsening dynamics C_{link} will be C independent for $C^2 < q^2_{\text{EA}}$ and large t_w (relevant system excitations are the spin reversal of compact droplets not affecting C_{link}), while in a RSB system new states are continuously found as time goes by: we expect a non constant C^2 dependence even if $C < q_{\text{EA}}$ [38].

By general arguments, the nonequilibrium C_{link} at finite *times* coincides with equilibrium correlation functions for systems of finite *size* [10]; see Fig. 3. We also predict the q^2 dependency of the *equilibrium* conditional expectation $Q_{\text{link}}|_q$ up to $L = 33$ [Q_{link} is just $C_4(r = 1)$, while q is the spatial average of $q_{\boldsymbol{x}}$, Eq. (3)].

As for the shape of the curve $C_{\text{link}} = f(C^2, t_w)$, Fig. 4 bottom, the t_w dependency is residual. Within our time window, C_{link} is not constant for $C < q_{\text{EA}}$. For comparison (inset) we show the qualitatively different curves for a coarsening dynamics. We studied the derivative $\mathrm{d}C_{\text{link}}/\mathrm{d}C^2$, for $C^2 < q^2_{\text{EA}}$, Fig. 4 top. We first smooth the curves by fitting $C_{\text{link}} = f(C^2)$ to the lowest order polynomial allowing a fair fit (seventh order for $t_w \leq 2^{25}$, sixth for larger t_w), whose derivative was taken afterwards (jackknife statistical errors).

Furthermore, we have extrapolated both $C_{\text{link}}(t = rt_w, t_w)$ and $C(t = rt_w, t_w)$ to $t_w \approx 10^{14}$ ($\sim$100 s), for $r = 8, 4, \ldots, \frac{1}{16}$ [39]. The extrapolated points for $t_w = 10^{14}$ fall on a straight line whose slope is plotted in the upper panel (thick line). The derivative is nonvanishing for $C^2 < q^2_{\text{EA}}$, for the experimental time scale.

In summary, Janus [30] halves the (logarithmic) time gap between simulations and nonequilibrium spin-glass experiments. We analyzed the simplest temperature quench, finding numerical evidence for a noncoarsening dynamics, at least up to experimental times (see also [27]). Let us highlight: *nonequilibrium* overlap equivalence (Figs. 3 and 4); nonequilibrium scaling functions reproducing *equilibrium* conditional expectations in finite systems

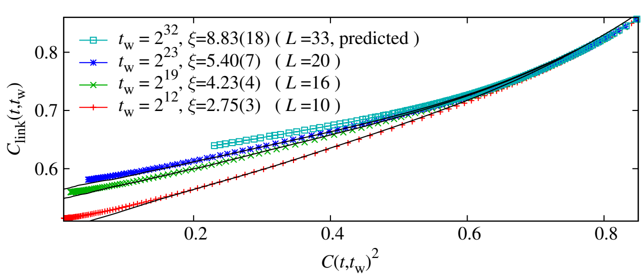

FIG. 3 (color online). For appropriate t_w and L, the nonequilibrium $C_{\text{link}}(t, t_w)$ vs $C^2(t, t_w)$ at $T = 0.7$, coincides with equilibrium $Q_{\text{link}}|_q$ vs q^2 (full lines, equilibrium data from [40] at $T = 0.7$, see text). From the length-time dictionary up to $L = 20$ we predict the equilibrium curve for $L = 33$.

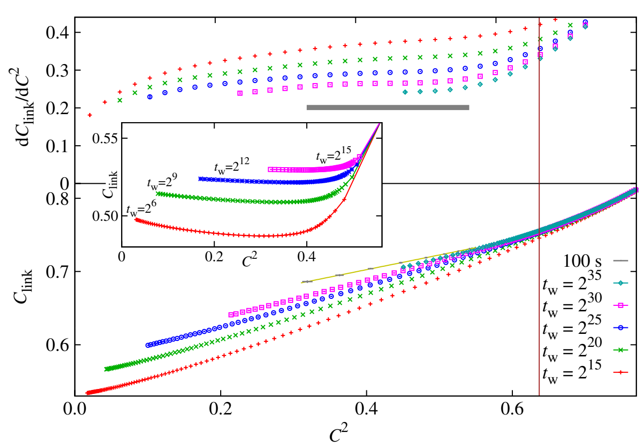

FIG. 4 (color online). Bottom: $C_{\text{link}}(t, t_w)$ vs $C^2(t, t_w)$ for $T = 0.6$ and some of our largest t_w (vertical line: q^2_{EA} from [24]). We also show our extrapolation of the C_{link} vs C^2 curve to $t_w = 10^{14}$ ($\sim$100 s, see text). Top: Derivative of C_{link} with respect to C^2 for $T = 0.6$. The horizontal line corresponds to the slope of a linear fit of $t_w = 10^{14}$ extrapolations (the line width equals twice the error). Inset: As in bottom panel, for the ferromagnetic site-diluted $D = 2$ Ising model (same simulation of Fig. 2).

(Fig. 3); and a nonequilibrium replicon exponent compatible with equilibrium computations [37]. The growth of the coherence length sensibly extrapolates to $t_w = 100$ s (our analysis of dynamic heterogeneities [26,27] will appear elsewhere [36]). Exploring with Janus nonequilibrium dynamics up to the *seconds* scale will allow the investigation of many intriguing experiments.

We corresponded with M. Hasenbusch, A. Pelissetto, and E. Vicari. Janus was supported by EU FEDER funds (UNZA05-33-003, MEC-DGA, Spain), and developed in collaboration with ETHlab. We were partially supported by MEC (Spain), through Contracts No. FIS2006-08533, FIS2007-60977, FPA2004-02602, TEC2007-64188; by CAM (Spain), and by Microsoft.

[1] J. A. Mydosh, *Spin Glasses: an Experimental Introduction* (Taylor and Francis, London, 1993).
[2] E. Vincent *et al.*, in *Lecture Notes in Physics*, edited by M. Rubí and C. Pérez-Vicente (Springer, New York, 1997), Vol. 492.
[3] G. F. Rodriguez, G. G. Kenning, and R. Orbach, Phys. Rev. Lett. **91**, 037203 (2003).
[4] V. Dupuis *et al.*, Pramana J. Phys. **64**, 1109 (2005).
[5] Y. G. Joh *et al.*, Phys. Rev. Lett. **82**, 438 (1999).
[6] F. Bert *et al.*, Phys. Rev. Lett. **92**, 167203 (2004).
[7] K. Gunnarsson *et al.*, Phys. Rev. B **43**, 8199 (1991).
[8] M. Palassini and S. Caracciolo, Phys. Rev. Lett. **82**, 5128 (1999).
[9] H. G. Ballesteros *et al.*, Phys. Rev. B **62**, 14237 (2000).
[10] S. Franz *et al.*, Phys. Rev. Lett. **81**, 1758 (1998); J. Stat. Phys. **97**, 459 (1999).
[11] W. L. McMillan, J. Phys. C **17**, 3179 (1984); A. J. Bray and M. A. Moore, in *Lecture Notes in Physics*, edited by J. L. van Hemmen and I. Morgensten (Springer, New York, 1987); D. S. Fisher and D. A. Huse, Phys. Rev. Lett. **56**, 1601 (1986); Phys. Rev. B **38**, 386 (1988).
[12] E. Marinari *et al.*, J. Stat. Phys. **98**, 973 (2000).
[13] F. Krzakala and O. C. Martin, Phys. Rev. Lett. **85**, 3013 (2000); M. Palassini and A. P. Young, Phys. Rev. Lett. **85**, 3017 (2000).
[14] G. Parisi and F. Ricci-Tersenghi, J. Phys. A **33**, 113 (2000).
[15] P. Contucci and C. Giardina, J. Stat. Phys. **126**, 917 (2007); Ann. Henri Poincaré **6**, 915 (2005).
[16] D. S. Fisher and D. A. Huse, Phys. Rev. B **38**, 373 (1988).
[17] Temperature chaos could still spoil the analogy [16].
[18] T. Temesvari, C. De Dominicis, and I. Kondor, J. Phys. A **27**, 7569 (1994).
[19] J. Kisker *et al.*, Phys. Rev. B **53**, 6418 (1996).
[20] H. Rieger, J. Phys. A **26**, L615 (1993).
[21] E. Marinari *et al.*, J. Phys. A **33**, 2373 (2000).
[22] L. Berthier and J.-P. Bouchaud, Phys. Rev. B **66**, 054404 (2002).
[23] S. Jimenez *et al.*, J. Phys. A **36**, 10 755 (2003).
[24] S. Perez Gaviro, J. J. Ruiz-Lorenzo, and A. Tarancón, J. Phys. A **39**, 8567 (2006).
[25] S. Jimenez, V. Martin-Mayor, and S. Perez-Gaviro, Phys. Rev. B **72**, 054417 (2005).
[26] L. C. Jaubert *et al.*, J. Stat. Mech. (2007) P05001; H. E. Castillo *et al.*, Phys. Rev. Lett. **88**, 237201 (2002); H. E. Castillo *et al.*, Phys. Rev. B **68**, 134442 (2003).
[27] C. Aron *et al.*, J. Stat. Mech. (2008) P05016.
[28] A. Cruz *et al.*, Comput. Phys. Commun. **133**, 165 (2001).
[29] A. Ogielski, Phys. Rev. B **32**, 7384 (1985).
[30] F. Belletti *et al.*, Comput. Sci. Eng. **8**, 41 (2006); Comput. Phys. Commun. **178**, 208 (2008); arXiv:0710.3535.
[31] M. Hasenbusch, A. Pelissetto, and E. Vicari, J. Stat. Mech. L02001 (2008); (private communication).
[32] See, e.g., D. J. Amit and V. Martin-Mayor, *Field Theory, the Renormalization Group and Critical Phenomena* (World-Scientific, Singapore, 2005), 3rd ed.
[33] Data at different t and t_w are correlated, so we consider only diagonal terms in the covariance matrix. Time correlations are considered by first forming jackknife blocks [32] (JKB) with the data for different samples, then minimizing this diagonal χ^2 for each JKB [23].
[34] See, e.g., A. D. Sokal, in *Functional Integration: Basics and Applications (Cargèse school 1996)*, edited by C. DeWitt-Morette, P. Cartier, and A. Folacci (Plenum, New Brunswick, 1997).
[35] We integrate $C_4(r, t_w)$ up to $r^{\text{cutoff}}(t_w)$, where $C_4(r^{\text{cutoff}}(t_w), t_w)$ becomes less than thrice its statistical error. We estimate the (small) remaining contribution, by fitting to (4) then integrating the fitted function from $r^{\text{cutoff}} - 1$ to $L/2$. Details will be given elsewhere [36].
[36] (Janus Collaboration) (to be published).
[37] E. Marinari and G. Parisi, Phys. Rev. Lett. **86**, 3887 (2001).
[38] $C_{\text{link}} = C^2$ in the full-RSB Sherrington-Kirkpatrick model.
[39] For each r, both the link and the spin correlation functions are independently fitted to $a_r + b_r t_w^{-c_r}$ (fits are stable for $t_w > 10^5$ with $c_r \approx 0.5$). These fits are then used to extrapolate the two correlation functions to $t_w = 10^{14}$.
[40] P. Contucci *et al.*, Phys. Rev. Lett. **99**, 057206 (2007); P. Contucci *et al.*, Phys. Rev. Lett. **96**, 217204 (2006).